ACS Infectious Diseases

Letter

Cite This: ACS Infect. Dis. 2018, 4, 1666−1670

pubs.acs.org/journal/aidcbc

Dual-Color Fluorescent Timer Enables Detection of Growth-Arrested Pathogenic Bacterium

Aiguo Xia,[†,∥] Jundong Han,[‡,∥] Zhenyu Jin,[†] Lei Ni,[†] Shuai Yang,[*,†] and Fan Jin[*,†,‡,§]

[†]Hefei National Laboratory for Physical Sciences at the Microscale, University of Science and Technology of China, No. 96, JinZhai Road Baohe District, Hefei, Anhui 230026, P. R. China

[‡]Department of Polymer Science and Engineering, University of Science and Technology of China, No. 96, JinZhai Road Baohe District, Hefei, Anhui 230026, P. R. China

[§]CAS Key Laboratory of Soft Matter Chemistry, University of Science and Technology of China, No. 96, JinZhai Road Baohe District, Hefei, Anhui 230026, P. R. China

Supporting Information

ABSTRACT: We present a method capable of detecting single slow-growing and growth-arrested cells in a bacterial culture composed of physiologically and phenotypically different cells. Unlike the use of transcriptional reporters to gauge the metabolic activities in cells, here, we fuse two different fluorescent proteins with distinctive maturation rates to construct a timer to directly determine the growth rate of single *Pseudomonas aeruginosa* cells. We demonstrate that the dual-color fluorescent timer can indicate the slow-growing and growth-arrested cells from bacterial cultures in the presence of various environmental stresses, including nutrient starvation or antibiotic treatments, which greatly expand the methods for detecting and isolating persister cells.

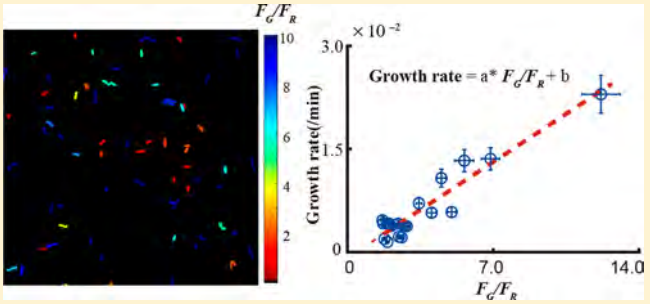

KEYWORDS: *fluorescent timer, pathogenic bacteria, persister cells*

Persisters constitute a subpopulation of genetically identical, but phenotypically various, bacterial cells that can survive different environmental stresses,[1,2] such as nutrient starvation or antibiotic exposure. Persister cells have been shown to have the ability to tolerate different medications.[3] Consequently, antibiotic treatments cannot completely eradicate bacterial cells in the nidus, which often results in the recalcitrance and relapse of persistent infections.[4] The therapies for persistent infections often involve repeated use of antibiotics, which has been shown to increase the risk of the emergence of antibiotic resistance.[5,6] Therefore, the understanding of persister cells has received broad attention.

Persister cells in bacteria are typically described as dormant, nondividing cells with globally reduced metabolism.[6−9] However, it is not clear what exactly a persister cell is or what the extent of dormancy is. Persister cells are not mutants, but phenotypic variants, of the wild type.[10] A significant aspect in understanding the persistence phenotype was the demonstration that cells exhibiting nongrowth or reduced growth rate are more likely to be persisters.[2,6,8,11] Cells in the persister state are highly immune to bacterial antibiotics, which are mainly caused by the slow growth of the persister cells.[12] Nongrowth or reduced growth rate makes perisister cells distinguishable. Persistence has been extremely difficult to research because persister subpopulations are a very small portion of the total bacteria population, for example, only one in one hundred thousand to one million cells of wild type *Escherichia coli* cells are persisters.[13] Hence, the method used to identify and isolate persister cells from a mixed population is crucial in persister research, in which fluorescent reporters play a significant role in the identification of persister cells because of their ability to monitor the physiological state at single-cell level. For example, Manina et al. constructed a transcriptional fluorescent reporter to monitor the ribosome production in *Mycobacterium tuberculosis*;[9] Helaine et al. constructed a fluorescent reporter based on fluorescence dilution to monitor the replication dynamics of *Salmonella typhimurium*.[14]

Given the fact that nongrowth or reduced growth rate is necessary and the most obvious characteristic of the persister cells, we here present a new approach to identify the slow-growing and growth-arrested single cells of an opportunistic pathogen, *Pseudomonas aeruginosa*, in a mixed population composed of physiologically and phenotypically different cells. We anticipate the application of such technologies for expanding the methods for detecting and isolating persister cells.

Briefly, we incorporated a designed module of a timer into the chromosome of *P. aeruginosa* with the mini-Tn7 system.[15] This fluorescent timer is a fusion of two fluorescent proteins with distinctive maturation rates (Figure S1): a red fluorescent

Received: May 29, 2018
Published: September 14, 2018

DOI: 10.1021/acsinfecdis.8b00129
ACS Infect. Dis. 2018, 4, 1666−1670

protein (Tdimer2)[16] with a slower maturation rate (τ_1 = 0.0058 min^{-1})[17] is fused to a green fluorescent protein (sfGFP) that possesses a much faster maturation rate (τ_2 = 0.1386 min^{-1}),[18] and the tandem protein is expressed using a constitutive promoter ($P_{A1/O4/O3}$). Notably, a fluorescent timer with a similar design was applied to investigate the protein dynamics in eukaryotic cells.[19] In contrast with eukaryotic cells, degradation of protein in the growing bacterial cell occurred at a very small rate, and the estimated minimum half-life for protein degradation in the bacteria is 30 days.[20] As a result, proteins are generally degraded on time scales that are significantly longer than the cell cycle, and most of the protein lifetime is controlled by a dilution due to cell division, whose time scale is equal to the cell cycle.[21,22] Therefore, the turnover of proteins in bacteria depends on only the growth rate of cells.[20−22] In line with the previous study, we further demonstrated that the fluorescent proteins, sfGFP and Tdimer2, in *P. aeruginosa* are stable and their lifetime is dominated by the rate of dilution due to cell division (Figure S2).

We assume that a fluorescent protein (FP) is produced at a constant rate as a nonfluorescent protein matures to a fluorescent protein with the corresponding maturation rate constant (τ). In our design, τ_1 is markedly slower than the optimized growth rate (μ = 0.0116 min^{-1}, i.e., doubling time = 60 min) of *P. aeruginosa*, whereas τ_2 is markedly faster than μ. Therefore, the red fluorescence (F_R) arising from Tdimer2 is strongly dependent on μ, because more Tdimer2 FPs can mature from nonfluorescent to fluorescent state in slow-growing or growth-arrested cells compared with normal-growing cells. The result is that the F_R arising from growth-arrested cells is much larger than the F_R arising from fast-growing cells. Conversely, the green fluorescence (F_G) arising from sfGFP is nearly independent of the μ because $\tau_2 \gg \mu$. The application of F_G/F_R is thereby expected to determine the actual growth rate of cells.

To calibrate the relationship between F_G/F_R and μ, we adjusted the concentration of the Fe^{3+} in the culture medium, which enabled us to change the average growth rate ($\langle\mu\rangle$) of cells from slow-growing to fast-growing (Figure S3). Afterward, we measured the ensemble average value of $\langle F_G/F_R\rangle$ in each growth condition. The sfGFP and Tdimer2 was excited using a 488 or 561 nm laser, respectively, and imaged with two different emission channels (524 or 607 nm). The captured fluorescent images were first subjected to field uneven excitations correction and background correction (See the Supporting Information). The corrected images arising from the sfGFP channel were further analyzed to obtain the bacterial contours using a standard image-processing algorithm coded by Matlab.[23] The fluorescent intensities of sfGFP or Tdimer2 arising from single cells (F_G or F_R) were determined by directly measuring averaged intensities of the pixels enclosed by bacterial contours. The ensemble average $\langle F_G/F_R\rangle$ was determined by averaging F_G/F_R arising from single cells. We determined that $\langle F_G/F_R\rangle$ was linearly related to the $\langle\mu\rangle$ and ranged from slow-growing ($\langle\mu\rangle$ = 0.0017 min^{-1}, doubling time = 400 min) to fast-growing conditions ($\langle\mu\rangle$ = 0.0230 min^{-1}, doubling time = 30 min) (Figure 1). To further elucidate this linear relation, we created a theoretical model to directly calculate the relation between F_G/F_R and μ (See the Supporting Information). The theoretical calculation accurately predicted the linear relation found in the experiments. These results conclusively demonstrated that the dual-color

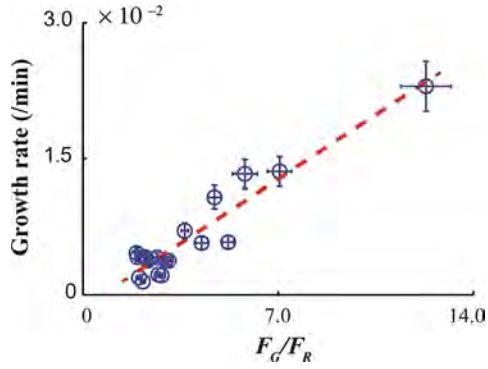

Figure 1. Linear relationship between average bacterial growth rate and average $\langle F_G/F_R\rangle$ in *P. aeruginosa*, where the red dashed line represents the linear fitting using a linear regress (growth rate = 0.002 × F_G/F_R − 0.001, R^2 = 0.89).

fluorescent timer can detect the slow-growing or growth-arrested bacteria. We also investigated the feasibility of the timer in *Pseudomonas putida*. The results showed that $\langle F_G/F_R\rangle$ was still linearly related to the $\langle\mu\rangle$ in these strains, which indicated the wide applicability of our designed fluorescent timer in bacteria cells (Figure S4).

Next, we used this fluorescent timer to identify the slow-growing and growth-arrested cells of *P. aeruginosa* in the presence of different environmental stresses, including nutrient starvation and low-dose treatment with aminoglycoside antibiotics ([tobramycin] = 2.0 $\mu g \cdot mL^{-1}$). The slow-growing and growth-arrested cells are defined here by 1.5 ≤ F_G/F_R < 6.0 (0.002 ≤ μ < 0.011 min^{-1} or 60 < doubling time ≤ 350 min) and 6.0 ≤ F_G/F_R (μ ≤ 0.002 min^{-1} or doubling time ≥ 350 min), respectively. To display the growth rate of single cells, we plotted the fluorescent intensities arising from the single cells at the plane defined by the F_G (*y*-axis) and the F_R (*x*-axis); one point in that plane represents one bacterium. We partitioned the plane of F_G and F_R using two lines with distinct slopes, that is, F_G/F_R = 1.5 (indicated by a red dashed line in Figures 2k−o and 3k−o) and F_G/F_R = 6.0 (indicated by a green dashed line in Figures 2k−o and 3k−o). The partition of the plane clearly indicated the growth state of the single cells because of the linear relation F_G/F_R and μ; namely, the points located in the regions between the green dashed line and the *y*-axis, between the green dashed line and the red dashed line, or between the red dashed line and the *x*-axis represent the fast-growing cells, slow-growing cells, or growth-arrested cells, respectively.

We collected the bacterial cultures at distinctive growth phases that ranged from early exponential to death phase, in which the nutrient availability declined during the planktonic culturing. The bacterial growth phases were defined using their growth curve (Figure S5): early exponential phase (0 < OD_{600} ≤ 0.9), later exponential phase (0.9 < OD_{600} ≤ 2), early stationary phase (2 < OD_{600} ≤ 2.2), later stationary phase (2 < OD_{600} ≤ 2.2), and death phase (OD_{600} ≤ 2), where OD_{600} was the optical density of bacterial cultures at 600 nm. We observed the following: (1) a small fraction of slow-growing cells (0.08%) was detected in the earlier exponential phase (Figure 2a,f,k); (2) a small fraction of growth-arrested cells (0.06%) was first detected in the later exponential phase (Figure 2b,g,l); (3) the percentage of slow-growing or growth-arrested cells increased from 23.32% to 99.19% (Figure 2c,h,m) or from 0.04% to 0.36% (Figure 2d,i,n) through the

DOI: 10.1021/acsinfecdis.8b00129
ACS Infect. Dis. 2018, 4, 1666−1670

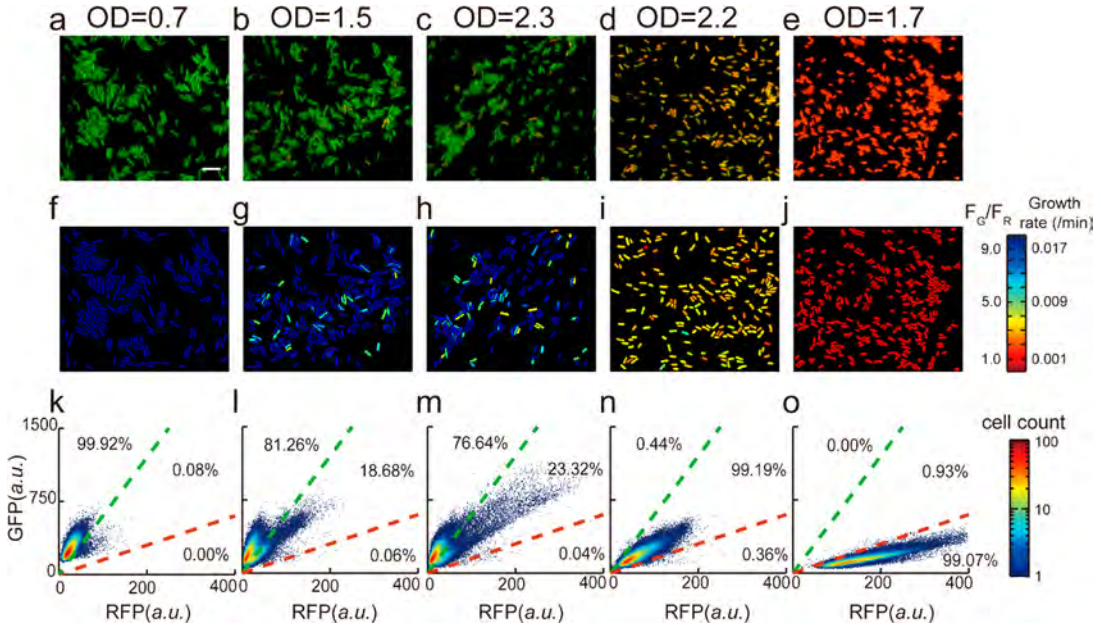

Figure 2. Dual-color fluorescent timer indicates the slow-growing or growth-arrested single cells of *P. aeruginosa* in planktonic culturing. (a–e) Merged representative fluorescent images show sfGFP (as indicated by green color) and Tdimer2 (as indicated by red color) intensities in the distinctive growth phase. (f–j) Representative ratio images show F_G/F_R in the distinctive growth phase, where the color map to the right of the panel j indicates the corresponding F_G/F_R or the growth rate in the images. (k–o) Relationship between the F_G and F_R in the distinctive growth phase, where the individual data points in the figures represent data arising from a single bacterium; green or red dashed lines represent the line with a slope of F_G/F_R = 6.0 (μ = 0.011/min) or F_G/F_R = 1.5 (μ = 0.002/min), respectively; color map to the right of panel o indicates the cell counts. (a,f,k), (b,g,l), (c,h,m), (d,i,n), and (e,j,o) represent the bacterial cultures harvested in the early exponential phase (OD_{600} = 0.7), later exponential phase (OD_{600} = 1.5), early stationary phase (OD_{600} = 2.3), later stationary phase (OD_{600} = 2.2), or death phase (OD_{600} = 1.7). Scale bars for all images are 4 μm.

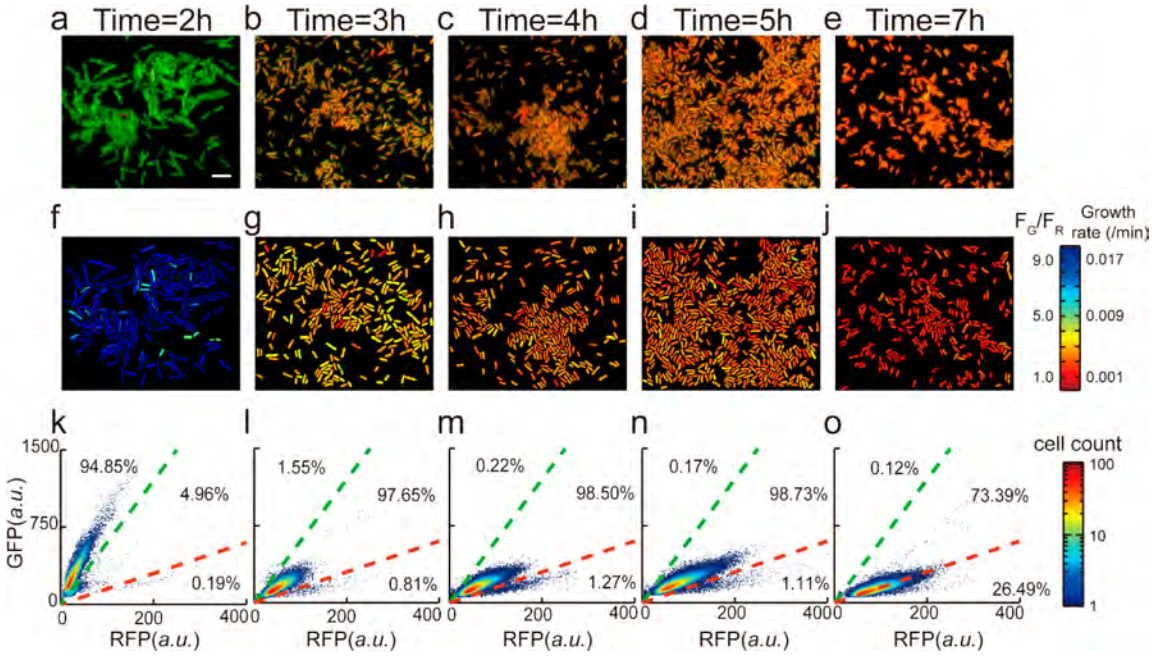

Figure 3. Dual-color fluorescent timer indicates the slow-growing or growth-arrested single cells of *P. aeruginosa* after the treatment of 2.0 μg mL^{-1} tobramycin. (a–e) Merged representative fluorescent images show sfGFP (as indicated by green color) and Tdimer2 (as indicated by red color) intensities after the treatment of 2 μg mL^{-1} tobramycin. (f–j) Representative ratio images show F_G/F_R after the treatment of tobramycin, where the color map to the right of the panel j indicates the corresponding F_G/F_R or the growth rate in the images. (k–o) Relationship between the F_G and F_R after the treatment of tobramycin, where the individual data points in the figures represent data arising from a single bacterium; green or red dashed lines represent the line with a slope of F_G/F_R = 6.0 (μ = 0.011/min) or F_G/F_R = 1.5 (μ = 0.002/min), respectively; color map to the right of the panel o indicates the cell counts. (a,f,k), (b,g,l), (c,h,m), (d,i,n), and (e,j,o) represent the bacterial cultures harvested in the different treatment times ranging from 2 to 7 h. Scale bars for all images are 4 μm.

DOI: 10.1021/acsinfecdis.8b00129
ACS Infect. Dis. 2018, 4, 1666–1670

stationary phase; (4) 0.93% of slow-growing cells consistently existed in the death phase (Figure 2e,j,o), and even the bacterial density declines at the population level. These results indicate that the bacterial cultures collected after the later exponential phase were actually composed of physiologically and phenotypically different cells, which implies that these physiologically and phenotypically different bacteria would respond differently to environmental cues, such as antibiotics treatments.

Next, we used low-dose tobramycin (2.0 $\mu g \cdot mL^{-1}$) to treat bacterial cultures collected in the exponential phase. Notably, 2.0 $\mu g \cdot mL^{-1}$ is the minimal inhibition concentration (MIC) of tobramycin for *P. aeruginosa*. We measured the F_G/F_R at different treatment times. We observed that (1) 4.96% slow-growing or 0.19% growth-arrested cells first appeared in the population after 2 h of treatment with tobramycin (Figure 3a,f,k); (2) 3−6 h of treatment with tobramycin led to the majority of *P. aeruginosa* cells (97.65−98.73%) remaining in a slow-growing state (Figure 3b−d,g−i,l−n) while 0.17−1.55% of cells remained in the fast-growing state; (3) 0.12% or 73.39% of cells remained in the fast- or slow-growing state, respectively, even after 8 h of treatment (Figure 3e,j,o). These results indicate that the majority of *P. aeruginosa* cells remained metabolically active after 8 h of exposure to 2.00 $\mu g \cdot mL^{-1}$ tobramycin, even though this condition can sufficiently inhibit the growth of *P. aeruginosa* at a population level.

In summary, we demonstrated that the application of a tandem fluorescent protein timer for analysis of bacterial growth rate does not require time-course measurements; it only needs snapshot fluorescence imaging, and further, the fluorescent timer can identify slow-growing and growth-arrested bacterial pathogens in a mixed population. Our results indicate that the ratio F_G/F_R, from the timer, is linearly related to the growth rate of cells in broad ranges. Such a linear relationship potentially enables the quantification of the growth of single cells in different scenarios, such as during the formation of biofilms. Furthermore, our calculation indicates the relation between the linear range and the growth rate depends on the maturation rate of a slower-maturing fluorescent protein, which enables the construction of a specific timer suitable for monitoring the growth of distinctive microbes on vastly different time scales with the use of a different red fluorescent protein that possesses a distinctive maturation rate. Specifically, the timer with the slower maturation rate of red fluorescent protein has a broader spectrum of time scales.[24] Established strategies for fluorescent protein evolution[25] can be used to broaden the spectrum of accessible time scales. For example, using lanRFP-ΔS83 (τ_1 = 0.0014 min^{-1})[26] to replace the Tdimer2 in the timer enables the identification of the dormant cells that may possess a much slower growth rate.

Compared with previously used fluorescent reporters that can also identify slow-growing and growth-arrested cells, the major advantages of this fluorescent timer are that (1) the output from the fluorescent timer is directly correlated to the growth rate of cells and (2) the inducer is not used to treat cells. Moreover, the fluorescent timer is fully compatible with the high-throughput techniques used to isolate cells, such as microfluidics or flow cytometry. These conveniences potentially enable the broad application of our fluorescent timer in persister-related studies.

■ ASSOCIATED CONTENT

Supporting Information

The Supporting Information is available free of charge on the ACS Publications website at DOI: 10.1021/acsinfecdis.8b00129.

Supplementary Experimental Section; Figure S1, schematic representation of the tandem fluorescent timer; Figure S2, turnover of fluorescent proteins in *P. aeruginosa* cells; Figure S3, growth curves of *P. aeruginosa* in the presence of different amounts of ferric; Figure S4, linear relationship between average bacterial growth rate and average $\langle F_G/F_R \rangle$ in *P. putida*; Figure S5, growth curve of *P. aeruginosa* in the presence of 1 μM $FeCl_3$ in the medium (PDF)

■ AUTHOR INFORMATION

Corresponding Authors

*E-mail: fjinustc@ustc.edu.cn. Tel.: +86-551-63606925. Fax: +86-551-63606743.

*E-mail: yssamber@mail.ustc.edu.cn. Tel.: +86-551-63606925. Fax: +86-551-63606743.

ORCID

Zhenyu Jin: 0000-0003-2733-867X

Fan Jin: 0000-0003-2313-0388

Author Contributions

‖A.X. and J.H. contributed equally to this work. F.J. conceived the project. Z.J. and A.X. performed the experiments. J.H. and L.N. prepared the fluorescent timer. Z.J., A.X., and S.Y. contributed jointly to data interpretation and manuscript preparation. F.J. and S.Y. wrote the manuscript. All authors have given approval to the final version of the manuscript.

Notes

The authors declare no competing financial interest.

■ ACKNOWLEDGMENTS

The National Natural Science Foundation of China (21474098, 21274141, 21522406, and 31700087) and the Fundamental Research Funds for the Central Universities (WK2340000066, WK2030020023, WK3450000003) supported this work.

■ REFERENCES

(1) Fisher, R. A., Gollan, B., and Helaine, S. (2017) Persistent bacterial infections and persister cells. *Nat. Rev. Microbiol. 15* (8), 453−464.

(2) Lewis, K. (2007) Persister cells, dormancy and infectious disease. *Nat. Rev. Microbiol. 5* (1), 48−56.

(3) Keren, I., Kaldalu, N., Spoering, A., Wang, Y., and Lewis, K. (2004) Persister cells and tolerance to antimicrobials. *FEMS Microbiol. Lett. 230* (1), 13−18.

(4) Helaine, S., Cheverton, A. M., Watson, K. G., Faure, L. M., Matthews, S. A., and Holden, D. W. (2014) Internalization of *Salmonella* by macrophages induces formation of nonreplicating persisters. *Science 343* (6167), 204−208.

(5) Lewis, K. (2008) Multidrug tolerance of biofilms and persister cells. *Curr. Top. Microbiol. Immunol. 322*, 107−131.

(6) Lewis, K. (2010) Persister cells. *Annu. Rev. Microbiol. 64*, 357−372.

(7) Shah, D., Zhang, Z., Khodursky, A., Kaldalu, N., Kurg, K., and Lewis, K. (2006) Persisters: a distinct physiological state of *E. coli*. *BMC Microbiol. 6*, 53.

DOI: 10.1021/acsinfecdis.8b00129
ACS Infect. Dis. 2018, 4, 1666−1670

(8) Kwan, B. W., Valenta, J. A., Benedik, M. J., and Wood, T. K. (2013) Arrested protein synthesis increases persister-like cell formation. *Antimicrob. Agents Chemother. 57* (3), 1468−1473.
(9) Manina, G., Dhar, N., and McKinney, J. D. (2015) Stress and host immunity amplify *Mycobacterium tuberculosis* phenotypic heterogeneity and induce nongrowing metabolically active forms. *Cell Host Microbe 17* (1), 32−46.
(10) Balaban, N. Q., Merrin, J., Chait, R., Kowalik, L., and Leibler, S. (2004) Bacterial persistence as a phenotypic switch. *Science 305* (5690), 1622−1625.
(11) Conlon, B. P., Rowe, S. E., and Lewis, K. (2015) Persister cells in biofilm associated infections. *Adv. Exp. Med. Biol. 831*, 1−9.
(12) Balaban, N. Q., Gerdes, K., Lewis, K., and McKinney, J. D. (2013) A problem of persistence: still more questions than answers? *Nat. Rev. Microbiol. 11* (8), 587−591.
(13) Kussell, E., Kishony, R., Balaban, N. Q., and Leibler, S. (2005) Bacterial persistence: a model of survival in changing environments. *Genetics 169* (4), 1807−1814.
(14) Helaine, S., Thompson, J. A., Watson, K. G., Liu, M., Boyle, C., and Holden, D. W. (2010) Dynamics of intracellular bacterial replication at the single cell level. *Proc. Natl. Acad. Sci. U. S. A. 107* (8), 3746−3751.
(15) Choi, K. H., and Schweizer, H. P. (2006) mini-Tn7 insertion in bacteria with single attTn7 sites: example *Pseudomonas aeruginosa*. *Nat. Protoc. 1* (1), 153−161.
(16) Vrzheshch, P. V., Akovbian, N. A., Varfolomeyev, S. D., and Verkhusha, V. V. (2000) Denaturation and partial renaturation of a tightly tetramerized DsRed protein under mildly acidic conditions. *FEBS Lett. 487* (2), 203−208.
(17) Shaner, N. C., Campbell, R. E., Steinbach, P. A., Giepmans, B. N., Palmer, A. E., and Tsien, R. Y. (2004) Improved monomeric red, orange and yellow fluorescent proteins derived from *Discosoma sp.* red fluorescent protein. *Nat. Biotechnol. 22* (12), 1567−1572.
(18) Pedelacq, J. D., Cabantous, S., Tran, T., Terwilliger, T. C., and Waldo, G. S. (2006) Engineering and characterization of a superfolder green fluorescent protein. *Nat. Biotechnol. 24* (1), 79−88.
(19) Khmelinskii, A., Keller, P. J., Bartosik, A., Meurer, M., Barry, J. D., Mardin, B. R., Kaufmann, A., Trautmann, S., Wachsmuth, M., Pereira, G., Huber, W., Schiebel, E., and Knop, M. (2012) Tandem fluorescent protein timers for in vivo analysis of protein dynamics. *Nat. Biotechnol. 30* (7), 708−714.
(20) Koch, A. L., and Levy, H. R. (1955) Protein turnover in growing cultures of *Escherichia coli*. *J. Biol. Chem. 217* (2), 947−957.
(21) Friedman, N., Cai, L., and Xie, X. S. (2006) Linking stochastic dynamics to population distribution: an analytical framework of gene expression. *Phys. Rev. Lett. 97* (16), 168302.
(22) Taniguchi, Y., Choi, P. J., Li, G. W., Chen, H., Babu, M., Hearn, J., Emili, A., and Xie, X. S. (2010) Quantifying *E. coli* proteome and transcriptome with single-molecule sensitivity in single cells. *Science 329* (5991), 533−538.
(23) Yang, S., Cheng, X., Jin, Z., Xia, A., Ni, L., Zhang, R., and Jin, F. (2018) Differential Production of Psl in Planktonic Cells Leads to Two Distinctive Attachment Phenotypes in *Pseudomonas aeruginosa*. *Appl. Environ. Microbiol. 84* (14), e00700-18.
(24) Khmelinskii, A., Keller, P. J., Bartosik, A., Meurer, M., Barry, J. D., Mardin, B. R., Kaufmann, A., Trautmann, S., Wachsmuth, M., Pereira, G., Huber, W., Schiebel, E., and Knop, M. (2012) Tandem fluorescent protein timers for in vivo analysis of protein dynamics. *Nat. Biotechnol. 30*, 708.
(25) Shaner, N. C., Patterson, G. H., and Davidson, M. W. (2007) Advances in fluorescent protein technology. *J. Cell Sci. 120* (24), 4247−4260.
(26) Pletnev, V. Z., Pletneva, N. V., Lukyanov, K. A., Souslova, E. A., Fradkov, A. F., Chudakov, D. M., Chepurnykh, T., Yampolsky, I. V., Wlodawer, A., Dauter, Z., and Pletnev, S. (2013) Structure of the red fluorescent protein from a lancelet (Branchiostoma lanceolatum): a novel GYG chromophore covalently bound to a nearby tyrosine. *Acta Crystallogr., Sect. D: Biol. Crystallogr. 69* (9), 1850−1860.

DOI: 10.1021/acsinfecdis.8b00129
ACS Infect. Dis. 2018, 4, 1666−1670